

# The Productions and Strong Decays of $D_q(2S)$ and $B_q(2S)$

Zhi-Hui Wang<sup>[1]</sup>, Guo-Li Wang<sup>[1,2]\*</sup>, Jin-Mei Zhang<sup>[3]</sup>, Tian-Hong Wang<sup>[1]</sup>

<sup>1</sup>*Department of Physics, Harbin Institute of Technology, Harbin, 150001, China*

<sup>2</sup>*PITT PACC, Department of Physics & Astronomy,  
University of Pittsburgh, PA 15260, USA*

<sup>3</sup>*Xiamen Institute of Standardization, Xiamen 361004, China*

## Abstract

We study the productions of first radial excited states  $D_q(2S)$  ( $q = u, d, s$ ) and  $B_q(2S)$  in exclusive semi-leptonic  $B_{q'}$  ( $q' = u, d, s, c$ ) decays by the improved Bethe-Salpeter method. These  $2S$  states can be detected through their strong decays to ground mesons, where the strong decays are calculated by the low energy approximation as well as the impulse approximation. Some channels have ratios of order  $10^{-4}$ :  $Br(B^+ \rightarrow \bar{D}^0(2S)\ell^+\nu_\ell) \times Br(\bar{D}^0(2S) \rightarrow \bar{D}^*\pi) \approx (4.9 \pm 4.0) \times 10^{-4}$ ,  $Br(B^0 \rightarrow D^-(2S)\ell^+\nu_\ell) \times Br(D^-(2S) \rightarrow \bar{D}^*\pi) \approx (4.4 \pm 3.4) \times 10^{-4}$ . These channels could be measured by the current B-factories. For  $D_s(2S)$ , we also obtain a relative large ratio:  $Br(B_s^0 \rightarrow D_s^-(2S)\ell^+\nu_\ell) \times Br(D_s^-(2S) \rightarrow \bar{D}^*\bar{K}) \approx (9.9 \pm 14.9) \times 10^{-4}$ . Although there are discrepancies of the full decay width between the theoretical predictions of  $D^0(2S)$  and experimental results of  $D(2550)^0$ , the new detected state  $D(2550)^0$  is very likely the  $D^0(2S)$  state.

**Keywords:** Radial excited  $D_q(2S)$  and  $B_q(2S)$  states; Semi-leptonic decay; Strong decay; Bethe-Salpeter method.

---

\* glwang@hit.edu.cn

## I. INTRODUCTION

In recent years, great progress has been made in hadronic mass spectra. There are many new states that have been observed, e.g., the new particles  $D_{s0}^*(2317)$  [1],  $D_{s1}(2700)$ ,  $D_{sJ}(2860)$  [2],  $\eta'_c$  [3],  $X(3872)$  [4],  $X(3940)$  [5],  $Y(3940)$  [6],  $Z(3930)$  [7] and  $Y(4260)$  [8]. Some of these new states are  $P$ -wave ( $L = 1$ ) state candidates, such as  $D_{s0}^*(2317)$ , and some of them are first radial excited  $2S$  ( $L = 0, n = 2$ ) state candidates, e.g.,  $D_{s1}(2700)$  and  $\eta'_c$ . Recently, other new  $2S$  state candidates  $D(2550)^0$  and  $D^*(2600)^0$  are observed in inclusive  $e^+e^-$  collisions near  $\sqrt{s} = 10.58$  GeV [9].

Besides the progress in experiment, there are many approaches to study the heavy excited states in theory, e.g., the authors of [10] considered  $B_c$  decays to excited  $2P$  and  $3S$  charmonium states with the relativistic quark model; the authors of [11] calculated the decay of  $B_c \rightarrow X_{c\bar{c}} l \nu_l$  where  $X_{c\bar{c}}$  was an excited charmonium state with the light-cone QCD sum rules approach; the authors of [12] used generalized factorization together with  $SU(3)_F$  symmetry to predict the branching ratios of  $B_s \rightarrow M_{c\bar{c}} + L$  where  $M_{c\bar{c}}$  was a charmonium state and  $L$  was a light scalar; using the ISGW2 quark model, and the authors of [13] studied  $B_c \rightarrow X_{c\bar{c}} M$  decays, where  $X_{c\bar{c}}$  was a radial excited charmonium  $\eta_c(2S)$  or  $\psi(2S)$ .

Although several papers considered the topics of radial excited  $2S$  states [14–17], there is still lack of theoretical investigation for the radial excited states  $D_q(2S)$  or  $B_q(2S)$ , where  $q$  is a light quark. One may also note that there is no other heavy-light  $2S$  state, which has ever been confirmed by the experiment except charmonium and bottomonium, this means we have little knowledge about heavy-light  $2S$  states, so the study of heavy-light  $2S$  states will enlarge our knowledge of bound states and QCD.

There are many methods to detect the heavy-light  $2S$  states experimentally. For example, by analyzing the inclusive productions of  $D^+\pi^-$ ,  $D^0\pi^+$  and  $D^{*+}\pi^-$  systems, the Babar collaboration found new mesons like  $D(2550)^0$  and  $D^*(2600)^0$  [9]. Since there are a large number of  $B$  data in two B-factories, and the LHC will produce large data of  $B_s$  and  $B_c$ , there will be a best and convenient way to detect heavy-light  $2S$  states by  $B_{q'}$  exclusive decays. In theory, the properties of the mesons were studied by many approaches together with the Dyson-Schwinger(DS) equation of QCD or the Bethe-Salpeter(BS) equation or both of them [18–20]. In this paper, we will study the productions of heavy-light  $2S$  states in exclusive semi-leptonic decays of  $B_{q'}$  mesons by the instantaneous approximate BS method [21, 22].

Knowing mass and life time (or full width) is helpful to detect the resonance experimen-

TABLE I: The total decay widths (in unit of MeV) of  $D(2550)^0$  treated as the  $D(2S)^0$  state; our results are estimated by the low energy approximation and the impulse approximation (in parentheses).

Ex [9]	this Paper	[23]	[24]	[25]	[26]	[27]
$130 \pm 12 \pm 13$	$43 \pm 23(47 \pm 17)$	8.4	8	22.1	124.1	45.35

tally. In a previous letter [23], we have studied mass and strong decay of some  $D_q(2S)$  and  $B_q(2S)$  states by the BS method. Unfortunately, there are large mass and width discrepancies between our predicted result of  $D^0(2S)$  and that of  $D(2550)^0$ , which is the candidate of  $D^0(2S)$  in the experiment [9]. Our predicted mass is 2.39 GeV of  $D^0(2S)$  [23], while Babar's result is  $2539.4 \pm 4.5 \pm 6.8$  MeV of  $D(2550)^0$  [9]. The total strong decay width of our calculation is 8.4 MeV (note that we missed a parameter 0.5 in all the strong decays whose final state involve  $\pi^0$ ), which is much smaller than the experimental value  $130 \pm 12 \pm 13$  MeV. There are several theoretical approaches to study the strong decays of this new state [23–28]. We show the theoretical estimated full decay widths and the experimental data in TABLE I. One can see that there are large discrepancies between experimental and theoretical results except the result of [26].

From our previous calculations, we find that there are three main reasons that result in discrepancies. First, we have chosen a simple potential—the Cornell potential—in order to reduce the difficulty of solving the BS equation, which is very complicated in this work. Second, we chose a group of old input parameters. Since there was no information of the  $2S$  state mass in the previous letter [23], we obtained the masses of  $2S$  states by fitting data of ground states with old parameters:  $m_b = 5.224$  GeV,  $m_c = 1.7553$  GeV,  $m_s = 0.487$  GeV,  $m_u \simeq m_d = 0.3$  GeV, and other parameters that character the potential [29]. Recently, by fitting data of charmonia and bottomonia which include higher excited states, and combining with the results of decay constants, we give new set of parameters:  $m_b = 4.96$  GeV,  $m_c = 1.62$  GeV,  $m_s = 0.5$  GeV,  $m_u \simeq m_d = 0.3$  GeV [21]. Third, our results are model dependent and we only consider two OZI-allowed channels to estimate the full decay width. Furthermore, the theoretical prediction of decay width is very sensitive to the mass of  $2S$  state.

In this paper, we focus on the decay and production of the  $2S$  states, not on the mass spectra, so we can vary the free parameter  $V_0$  to obtain the new mass spectra in TABLE II and the numerical values of wavefunctions, which are used to calculate the transition matrix

elements in appendix B. By varying all the input parameters simultaneously within 5% of central values, we obtain the uncertainties of masses in TABLE II.

Although we focus on the production of heavy-light  $2S$  states in the semi-leptonic decays of  $B_{q'}$ , we would like to re-calculate their strong decays by the re-predicted mass spectra. The strong decay widths are very sensitive to the kinematic range, so some new strong decay channels with higher mass of  $2S$  states can exist, e.g., there is a strong decay with a  $P$ -wave state involved in final states. Finally, we calculate the ratios of strong decays to reduce the effect of model dependence, and estimate the production ratios of  $B_{q'}$  semi-leptonic decay to the first radial excited states, which are reconstructed by the ground particles in terms of strong decay.

The rest of the paper is organized as follows. In section II, we show the formulations of semi-leptonic and strong decays. We give the hadronic matrix elements of semi-leptonic and strong decays in section III. The results and discussions are given in section IV. In the appendices we introduce BS equation and give some necessary formulas for the calculations of semi-leptonic and strong decays.

## II. THE FORMULATIONS OF SEMI-LEPTONIC DECAYS AND STRONG DECAYS

In this section, we present the formulations of  $B_{q'}$  mesons semi-leptonic decay to  $2S$  mesons and the strong decays of  $2S$  mesons.

### A. Semi-leptonic decay of $B_{q'}$

As we mentioned previously, the best way to study  $2S$  state is through the exclusive semi-leptonic decay of initial heavy meson ( $B^0$ ,  $B^+$ ,  $B_s^0$  or  $B_c$ ). Here, we take the  $B^0 \rightarrow D^-(2S)\ell^+\nu_\ell$  (see figure 1) as an example to show the formulation. The amplitude of this process is

$$T = \frac{G_F}{\sqrt{2}} V_{cb} \bar{u}_{\nu_\ell} \gamma^\mu (1 - \gamma_5) v_\ell \langle D_{2S}^-(P_f) | J_\mu | B^0(P) \rangle, \quad (1)$$

where  $V_{cb}$  is the CKM matrix element,  $J_\mu = V_\mu - A_\mu$  is the charged weak current, and  $P$  and  $P_f$  are the momentum of the initial meson  $B^0$  and the final state  $D^-(2S)$ , respectively. The hadronic part can be written as

$$\langle D_{2S}^-(P_f) | V_\mu | B^0(P) \rangle = f_+(P + P_f)_\mu + f_-(P - P_f)_\mu,$$

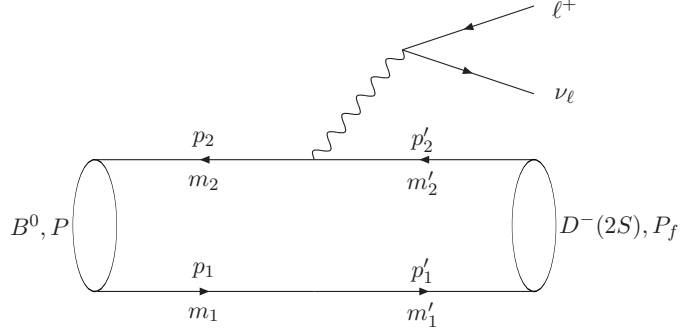


FIG. 1: Feynman diagram of the semi-leptonic decay  $B^0 \rightarrow D^-(2S)\ell^+\nu_\ell$ .

$$\langle D_{2S}^-(P_f) | A_\mu | B^0(P) \rangle = 0, \quad (2)$$

where  $f_+$ ,  $f_-$  are the Lorentz invariant form factors.

We define  $x \equiv E_\ell/M$ ,  $y \equiv (P - P_f)^2/M^2$ , where  $E_\ell$  is the energy of the final charge lepton and  $M$  is the mass of initial meson. The differential width of the decay can be reduced to

$$\begin{aligned} \frac{d^2\Gamma}{dx dy} &= |V_{bc}|^2 \frac{G_F^2 M^5}{64\pi^3} \\ &\left\{ \beta_{++} \left[ 4 \left( 2x \left( 1 - \frac{M_f^2}{M^2} + y \right) - 4x^2 - y \right) + \frac{m_\ell^2}{M^2} \left( 8x + 4 \frac{M_f^2}{M^2} - 3y - \frac{m_\ell^2}{M^2} \right) \right] \right. \\ &\left. (\beta_{+-} + \beta_{-+}) \frac{m_\ell^2}{M^2} \left( 2 - 4x + y - 2 \frac{M_f^2}{M^2} + \frac{m_\ell^2}{M^2} \right) + \beta_{--} \frac{m_\ell^2}{M^2} \left( y - \frac{m_\ell^2}{M^2} \right) \right\}, \quad (3) \end{aligned}$$

where  $M_f$ ,  $m_\ell$  are the masses of the meson and the lepton in final, respectively.  $\beta_{++} = f_+^2$ ,  $\beta_{+-} = \beta_{-+} = f_+ f_-$ ,  $\beta_{--} = f_-^2$ .

## B. Strong decay of $2S$ mesons

As an example, we consider the OZI-allowed strong decay  $D^-(2S) \rightarrow \bar{D}^{*0}\pi^-$  (see figure 2). In this work, we take the instantaneous approximation for the interaction kernel in meson; it is fit to describe the double heavy mesons ( $B_c, \eta_c$ ) and heavy-light mesons ( $D_q, B_q$ ) [30, 31], but it is inapplicable to double light meson ( $K, \pi$ ), which have complicated internal structure. In this work, we take the reduction formula, PCAC relation and low energy theorem to deal with the strong decay as we did in [32]. The strong decay amplitude of figure 2 can be written as [23, 32]

$$T = \frac{P_{f_2}^\mu}{f_{P_{f_2}}} \langle \bar{D}^{*0}(P_{f_1}) | \bar{u} \gamma_\mu \gamma_5 d | D_{2S}^-(P_f) \rangle, \quad (4)$$

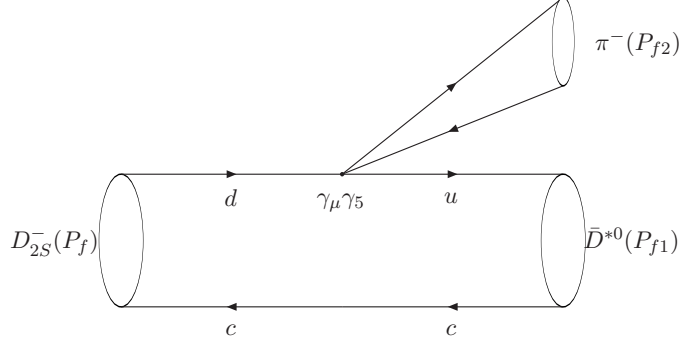


FIG. 2: Feynman diagram of strong decay  $D^-(2S) \rightarrow \bar{D}^{*0}\pi^-$  (low-energy approximation).

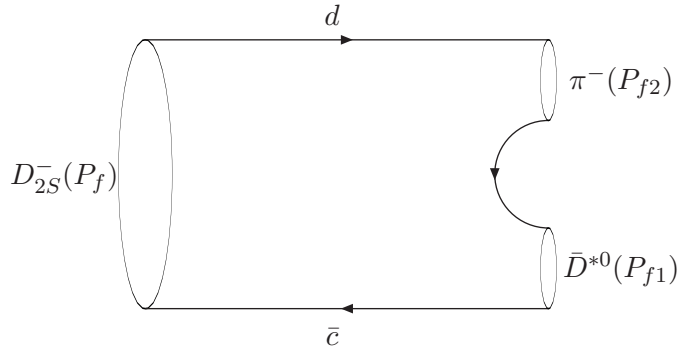


FIG. 3: Feynman diagram of strong decay  $D^-(2S) \rightarrow \bar{D}^{*0}\pi^-$  (impulse approximation).

where  $P_f$ ,  $P_{f1}$  and  $P_{f2}$  are the momenta of the  $D^-(2S)$ , final states  $\bar{D}^{*0}$  and  $\pi^-$ , respectively,  $f_{P_{f2}}$  is the decay constant of  $\pi^-$ ; we call this method the low energy approximation in this paper.

As a comparison, we also calculate the strong decays using an alternative method called the impulse approximation [33, 34]. According to this method, the decay amplitude of  $D^-(2S) \rightarrow \bar{D}^{*0}\pi^-$  can be written as (see Fig. 3)

$$T = \int \frac{d^4 q_f d^4 q_{f1}}{(2\pi)^4} \text{Tr} \left\{ S_1(p'_1) \eta_{P_f}(q_f) S_2(p'_2) \bar{\eta}_{P_{f1}}(q_{f1}) S'_1(p''_1) \Gamma_\pi(P_{f2}) \delta^4(\alpha'_2 P_f - q_f - (\alpha''_2 P_{f1} - q_{f1})) \right\}, \quad (5)$$

where  $q_f$ ,  $q_{f1}$  are the relative momentum of quark-anti-quark in  $D^-(2S)$  and  $\bar{D}^{*0}$ ,  $S_1(p'_1)$ ,  $S_2(p'_2)$  and  $S'_1(p''_1)$  are propagators,  $\eta_{P_f}(q_f)$ ,  $\bar{\eta}_{P_{f1}}(q_{f1})$  are the heavy-meson BS amplitudes, respectively;  $p'_1 = \alpha'_1 P_f + q_f$ ;  $p'_2 = \alpha'_2 P_f - q_f$ ;  $p''_1 = \alpha''_1 P_{f1} + q_{f1}$ ;  $\alpha'_1 = \frac{m_d}{m_d + m_c}$ ;  $\alpha'_2 = \frac{m_c}{m_d + m_c}$ ;  $\alpha''_1 = \frac{m_u}{m_u + m_c}$ ; and  $\alpha''_2 = \frac{m_c}{m_u + m_c}$ .  $\Gamma_\pi(P_{f2})$  is the BS amplitude of  $\pi$ .

After instantaneous approximation, equation (5) can be written as

$$T = \int \frac{d^3q_f}{(2\pi)^3} Tr \left\{ \varphi_{P_f}^{++}(q_{f\perp}) \frac{\not{P}_f}{M_f} \bar{\varphi}_{P_{f1}}^{++}(q_{f1\perp}) \Gamma_\pi(q_{f\perp}; P_{f2}) \right\}, \quad (6)$$

where  $q_{f\perp} = (0, \vec{q}_f)$ ,  $q_{f1\perp} = q_{f\perp} + \frac{m_c}{m_c+m_u} P_{f1\perp}$ ,  $\varphi_{P_f}^{++}(q_{f\perp})$  is the positive energy wavefunction for  $D_{2S}^-(P_f)$ .  $\varphi_{P_{f1}}^{++}(q_{f1\perp})$  is the positive energy wavefunction for  $\bar{D}^{*0}$ .  $\Gamma_\pi(q_{f\perp}; P_{f2}) = i\gamma_5 \frac{\sqrt{2}}{f_\pi} B_\pi(q_{f\perp}^2)$ ; one can find detailed calculation of  $B_\pi(q_{f\perp}^2)$  in [33–35].

There are two channels for the  $D^-(2S)$  meson:  $D^-(2S) \rightarrow \bar{D}^{*0}\pi^-$  ( $0^-(2S) \rightarrow 1^-0^-$ ) and  $D^-(2S) \rightarrow \bar{D}_0^*(2400)^0\pi^-$  ( $0^-(2S) \rightarrow 0^+0^-$ ). The strong decay amplitudes can be described by the strong coupling constants

$$\begin{aligned} T(D^-(2S) \rightarrow \bar{D}^{*0}\pi^-) &= G_{D^-(2S)\bar{D}^{*0}\pi}(\varepsilon^{(\lambda)} \cdot P_f), \\ T(D^-(2S) \rightarrow \bar{D}_0^*(2400)^0\pi^-) &= G_{D^-(2S)\bar{D}_0^*\pi}, \end{aligned} \quad (7)$$

where  $G_{D^-(2S)\bar{D}^{*0}\pi}$  and  $G_{D^-(2S)\bar{D}_0^*\pi}$  are the strong coupling constants, and  $\varepsilon$  is the polarization vector of meson  $\bar{D}^{*0}$ .

With equation (7), we obtain the decay widths

$$\begin{aligned} \Gamma_{D^-(2S)\bar{D}^{*0}\pi} &= \frac{|\vec{P}_{f1}|}{8\pi M_f^2} \sum_\lambda |T(D^-(2S) \rightarrow \bar{D}^{*0}\pi^-)|^2, \\ \Gamma_{D^-(2S)\bar{D}_0^*(2400)^0\pi^-} &= \frac{|\vec{P}_{f1}|}{8\pi M_f^2} |T(D^-(2S) \rightarrow \bar{D}_0^*(2400)^0\pi^-)|^2. \end{aligned} \quad (8)$$

From equations (1) and (4), we find that the main task of semi-leptonic and strong decay is to calculate the amplitudes  $\langle D_{2S}^-(P_f) | J_\mu | B^0(P) \rangle$  and  $\langle \bar{D}^{*0}(P_{f1}) | \bar{u}\gamma_\mu\gamma_5 d | D_{2S}^-(P_f) \rangle$ .

### III. THE HADRONIC MATRIX ELEMENTS OF SEMI-LEPTONIC DECAY AND STRONG DECAY

#### A. Hadronic matrix element of semi-leptonic decay

The calculation of the hadronic matrix element are different from model to model. In this paper, we combine the BS method that is based on the relativistic BS equation with the Mandelstam formalism [36] and relativistic wavefunctions to calculate the hadronic matrix element. The numerical values of wavefunctions have been obtained by solving the full Salpeter equation that we have introduced in the appendices. As an example, we consider

the semi-leptonic decay  $B^0 \rightarrow D^-(2S)\ell^+\nu_\ell$ . In this way, at the leading order, the hadronic matrix element can be written as [22]

$$\langle D_{2S}^-(P_f) | J_\mu | B^0(P) \rangle = \int \frac{d\vec{q}}{(2\pi)^3} \text{Tr} \left[ \bar{\varphi}_{P_f}^{++}(\vec{q}_f) \frac{\not{P}}{M} \varphi_P^{++}(\vec{q}) \gamma_\mu (1 - \gamma_5) \right], \quad (9)$$

where  $\vec{q}$  ( $\vec{q}_f$ ) is the relative three-momentum between the quark and the anti-quark in the initial (final) meson and  $\vec{q}_f = \vec{q} - \alpha_1' \vec{r}$ .  $M$  is the mass of  $B^0$ ,  $\vec{r}$  is the three-dimensional momentum of  $D^-(2S)$ ,  $\varphi_P^{++}(\vec{q})$  is the positive Salpeter wavefunction of  $B^0$  meson and  $\varphi_{P_f}^{++}(\vec{q}_f)$  is the positive Salpeter wavefunction of  $D^-(2S)$  meson,  $\bar{\varphi}_{P_f}^{++} = \gamma_0(\varphi_{P_f}^{++})^\dagger \gamma_0$ . We have given the Salpeter wavefunctions for the different mesons and form factors in appendix B.

## B. Hadronic matrix element of strong decays

We have obtained the amplitude of strong decay  $D^-(2S) \rightarrow \bar{D}^{*0}\pi^-$  in equation (4), and the key factor is to calculate the hadronic matrix element  $\langle \bar{D}^{*0}(P_{f1}) | \bar{u}\gamma_\mu\gamma_5 d | D_{2S}^-(P_f) \rangle$ . The hadronic matrix element  $\langle \bar{D}^{*0}(P_{f1}) | \bar{u}\gamma_\mu\gamma_5 d | D_{2S}^-(P_f) \rangle$  can be written as [32]

$$\langle \bar{D}^{*0}(P_{f1}) | \bar{u}\gamma_\mu\gamma_5 d | D_{2S}^-(P_f) \rangle = \int \frac{d\vec{q}_f}{(2\pi)^3} \text{Tr} \left[ \bar{\varphi}_{P_{f1}}^{++}(\vec{q}_{f1}) \gamma_\mu \gamma_5 \varphi_{P_f}^{++}(\vec{q}_f) \frac{\not{P}_f}{M_f} \right]. \quad (10)$$

We give the relation of wavefunctions and the strong coupling constants of different strong decays in appendix B.

## IV. NUMBER RESULTS AND DISCUSSIONS

### A. Semi-leptonic decays

In order to fix the Cornell potential in equation (A11) and masses of quarks, we take these parameters:  $a = e = 2.7183$ ,  $\lambda = 0.21 \text{ GeV}^2$ ,  $\Lambda_{QCD} = 0.27 \text{ GeV}$ ,  $\alpha = 0.06 \text{ GeV}$ ,  $m_b = 4.96 \text{ GeV}$ ,  $m_c = 1.62 \text{ GeV}$ ,  $m_s = 0.5 \text{ GeV}$ ,  $m_u = 0.305 \text{ GeV}$ ,  $m_d = 0.311 \text{ GeV}$ , *etc* [21], which are best to fit the mass spectra of ground states  $D_q$ ,  $B_q$  and other heavy mesons. In the previous letter [23], we have obtained masses of ground states and  $2S$  states by solving the BS equation. But we find that the mass of  $D^0(2S)$  in [23] is smaller than the one of  $D(2550)^0$ . In order to fit the experimental value of  $D(2550)^0$ , we change the free parameter  $V_0(D^0)$  to  $V_0(D^0(2S))$ . For other heavy-light  $2S$  states that do not have experimental data, we vary  $V_0(1S)$  that has the same value as  $\Delta V_0 = V_0(D^0(2S)) - V_0(D^0)$  to obtain the masses



TABLE II: Masses of the  $1S$  and  $2S$  states (in unit of MeV), ‘Ex’ means the experimental data from PDG [37] and [9], ‘Th’ means our prediction.

	Th	Ex		Th	Ex
$D^-(1S)$	1869.4	1869.6±0.16	$\bar{D}^0(1S)$	1865.0	1864.83±0.14
$D^-(2S)$	2560 ± 110		$\bar{D}^0(2S)$	2550 ± 109	2539.4 ± 4.5 ± 6.8 [9]
$M(2S) - M(1S)$	691 ± 110		$M(2S) - M(1S)$	685 ± 109	674.6 ± 4.5 ± 6.8
$B^0(1S)$	5279.5	5279.5±0.3	$D_s^-(1S)$	1968.2	1968.47±0.33
$B^0(2S)$	5930 ± 279		$D_s^-(2S)$	2641 ± 123	
$M(2S) - M(1S)$	651 ± 279		$M(2S) - M(1S)$	673 ± 123	
$B^+(1S)$	5279.0	5279.17±0.29	$B_s^0(1S)$	5367.9	5366.3±0.6
$B^+(2S)$	5930 ± 280		$B_s^0(2S)$	6020 ± 281	
$M(2S) - M(1S)$	651 ± 280		$M(2S) - M(1S)$	652 ± 281	

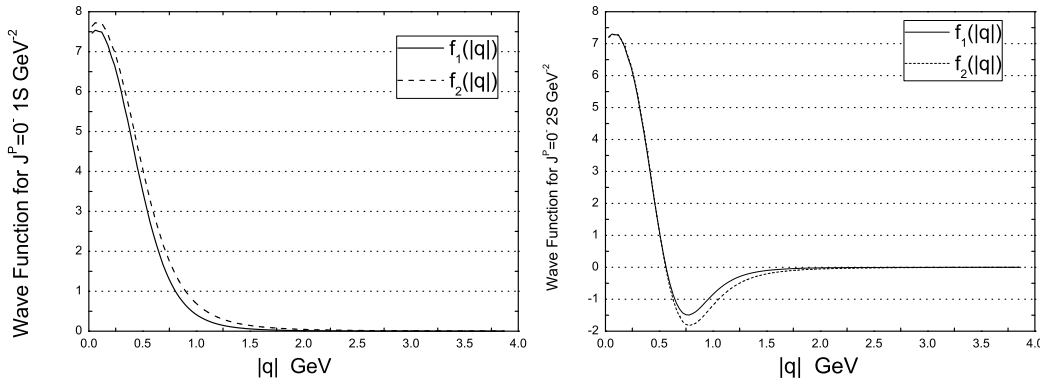


FIG. 4: The wavefunctions of  $1S$  and the  $2S$  of  $D^-$  meson with  $J^P = 0^-$ .

spectra of other heavy-light  $2S$  states. Then, we obtain the mass spectra of different mesons in TABLE II. Varying all the input parameters( $\lambda$ ,  $\Lambda_{QCD}$ , *etc*) simultaneously within 5% of the central values, we obtain the uncertainties of masses. To show the numerical results of wavefunctions explicitly, we plot the wavefunctions of  $1S$  and  $2S$  states for  $D^-$  meson with  $J^P = 0^-$  in figure 4. For semi-leptonic decays, we need to input the CKM matrix elements:  $V_{cb} = 0.0406$ ,  $V_{cd} = 0.23$ ,  $V_{cs} = 0.97334$  and the lifetimes of mesons:  $\tau_{B^0} = 1.53 \times 10^{-12}s$ ,  $\tau_{B^+} = 1.638 \times 10^{-12}s$ ,  $\tau_{B_c} = 0.453 \times 10^{-12}s$ ,  $\tau_{B_s^0} = 1.47 \times 10^{-12}s$ , which are taken from PDG [37].

In figure 5, as an example, we plot the form factors of the decay  $B^0 \rightarrow D^-(2S)\ell^+\nu_\ell$ , as

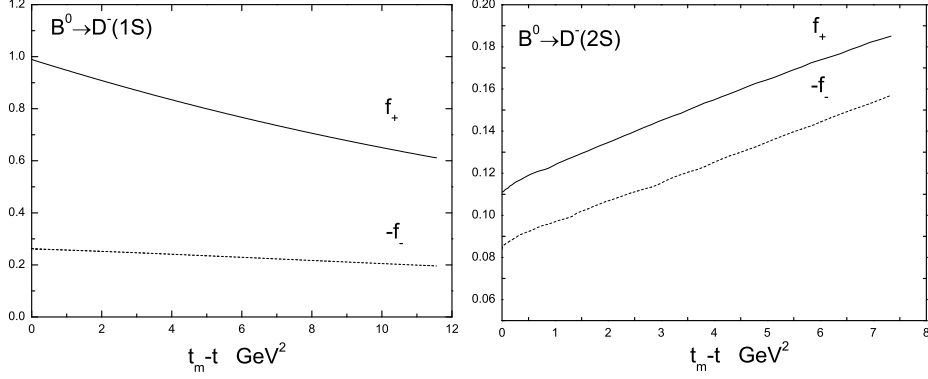


FIG. 5: The form factors of  $B^0 \rightarrow D^-(1S)\ell^+\nu_\ell$  and  $B^0 \rightarrow D^-(2S)\ell^+\nu_\ell$ .

TABLE III: The decay widths and branching ratios of exclusive semi-leptonic decay modes.

Modes	$\Gamma$ ( $10^{-16}$ GeV)	Br ( $10^{-4}$ )	Modes	Br (%)
$B^+ \rightarrow \bar{D}^0(2S)\ell^+\nu_\ell$	$2.05 \pm 0.61$	$5.1 \pm 1.5$	$B^+ \rightarrow \bar{D}^0(1S)\ell^+\nu_\ell$	$1.4 \sim 2.2$ [38]
$B^0 \rightarrow D^-(2S)\ell^+\nu_\ell$	$1.95 \pm 0.54$	$4.5 \pm 1.3$	$B^0 \rightarrow D^-(1S)\ell^+\nu_\ell$	$1.3 \sim 2.0$ [38]
$B_s^0 \rightarrow D_s^-(2S)\ell^+\nu_\ell$	$4.3 \pm 1.2$	$9.9 \pm 2.7$	$B_s^0 \rightarrow D_s^-(1S)\ell^+\nu_\ell$	$1.4 \sim 1.7$ [30]
$B_c^+ \rightarrow B^0(2S)\ell^+\nu_\ell$	$0.0171 \pm 0.0086$	$0.0120 \pm 0.0060$	$B_c^+ \rightarrow B^0(1S)\ell^+\nu_\ell$	$0.090 \sim 0.11$
$B_c^+ \rightarrow B_s^0(2S)\ell^+\nu_\ell$	$0.052 \pm 0.023$	$0.037 \pm 0.016$	$B_c^+ \rightarrow B_s^0(1S)\ell^+\nu_\ell$	$1.2 \sim 1.6$

a comparison, and we also show the form factors of  $B^0 \rightarrow D^-(1S)\ell^+\nu_\ell$  in the same method, where  $t = (P - P_f)^2 = M^2 + M_f^2 - 2ME_f$  and  $t_m$  is the maximum of  $t$ . One can see that the values of form factors of  $B^0 \rightarrow D^-(2S)$  are much smaller than that of  $B^0 \rightarrow D^-(1S)$ , and they have different shapes in figures. The reasons of these differences, especially the different shape, are mainly caused by the different wavefunctions of  $1S$  and  $2S$  states shown in figure 4; the numerical values of the wavefunctions for  $D^-(1S)$  are positive and decrease along with the increased momentum  $|q|$ , while there is a node structure in  $D^-(2S)$  wavefunction, after the node, the wavefunctions are negative, and whose negative values increase along with momentum  $|q|$ . This negative part wavefunctions are responsible for the small decay width and special shape of form factors; similar behaviors of the form factors are also obtained in [16, 17].

In TABLE III, we show the semi-leptonic decay widths and branching ratios with final mesons being  $2S$  states, also the ones of corresponding  $1S$  states in the same method for comparison. With the same initial particle and same CKM matrix element values, the branching

ratios of the  $2S$  channels are much smaller than the ones of the  $1S$  channels. This can be understood by the differences of phase spaces and the node structure of wavefunctions of  $2S$  state. The uncertainties of masses and decay widths shown in TABLE II and TABLE III are very large, some of them are almost 30%. The large uncertainties not only come from the uncertainties of phase spaces, but also from the variation of the node of the  $2S$  wave function, that means a little change of node location will result in large uncertainties.

Although compared with ground-state cases, the production ratios of  $2S$  states are very small, the branching ratios of  $B^0 \rightarrow D^-(2S)\ell^+\nu_\ell$  and  $B^+ \rightarrow \bar{D}^0(2S)\ell^+\nu_\ell$  around  $10^{-3} \sim 10^{-4}$  are very considerable. They are much larger than that of some rare decay modes and are accessible in the current  $B$  decay data. For the channel of  $B_s^0 \rightarrow D_s^-(2S)\ell^+\nu_\ell$ , the branching ratio of order  $10^{-3}$  can also be accessible in the near future. But for the case of  $B_c^+ \rightarrow B^0(2S)\ell^+\nu_\ell$ , due to the small  $V_{cd}$  and the phase space, we obtain narrow decay width and small branching ratio. For the decay  $B_c^+ \rightarrow B_s^0(2S)\ell^+\nu_\ell$ ,  $V_{cs}$  is large, while the phase space is very small, so the decay rate is small too. We also point out that small phase space and the node structure result in almost 50% uncertainties for the channels of  $B_c^+ \rightarrow B^0(2S)\ell^+\nu_\ell$  and  $B_c^+ \rightarrow B_s^0(2S)\ell^+\nu_\ell$ .

## B. Strong decays

These heavy-light  $2S$  states can be detected experimentally through their strong decays. In the previous letter, we have calculated the strong decays of some  $2S$  mesons [23]. But the predicted mass of  $D^0(2S)$  is smaller than the experimental data of  $D(2550)^0$ , which we have analyzed the reasons in the introduction, so we got narrow widths of  $B_q(2S)$  and  $D_q(2S)$  in terms of their OZI-allowed strong decays. In this paper, taking new parameters, we re-calculate the strong decays of  $B_q(2S)$  and  $D_q(2S)$  with large masses. For example, we calculate the strong decay  $D^{*-} \rightarrow \bar{D}^0\pi^-$  by the low-energy approximation, as well as the impulse approximation, and obtain the strong coupling constant  $G_{D^*D\pi}=19.8(18.3)^1$ , which is very closed to the experimental value  $G_{D^*D\pi} = 17.9 \pm 0.3 \pm 1.9$  [39] and the result of quenched lattice QCD calculation  $G_{D^*D\pi} = 18.8 \pm 2.3_{-2.0}^{+1.1}$  [40]. For  $B^{*0} \rightarrow B^+\pi^-$ , which is phase space suppressed, but as one more test of our method, similar to [33, 41, 42], we consider final  $\pi$  as a soft-pion, and obtain the strong coupling constant  $G_{B^*B\pi}=52.7(37.2)^1$ ,

---

<sup>1</sup> The first value come from the low-energy approximation, and the value in parentheses comes from the impulse approximation.

the impulse approximation result 37.2 is close to the same method result  $G_{B^*B\pi} = 30.0_{-1.4}^{+3.2}$  in [33], but come with a discrepancy may come from the further instantaneous approach. Then, for the first radial excited states, we calculate the transition matrix elements of the strong decay channels,  $0^-(2S) \rightarrow 1^-0^-, 0^+0^-$ , and obtain the strong coupling constants<sup>1</sup>:

$$\begin{aligned}
G_{\bar{D}^0(2S)\bar{D}^{*0}\pi^0} &= 3.71 \pm 0.10(3.96 \pm 0.34), & G_{\bar{D}^0(2S)D^{*-}\pi^+} &= 5.24 \pm 0.25(5.62 \pm 0.45), \\
G_{\bar{D}^0(2S)\bar{D}_0^{*0}\pi^0} &= 0.82 \pm 0.13(0.340 \pm 0.032) \text{ GeV}, & G_{\bar{D}^0(2S)D_0^{*-}\pi^+} &= 1.10 \pm 0.33(0.58 \pm 0.15) \text{ GeV}, \\
G_{D^-(2S)D^{*-}\pi^0} &= 3.71 \pm 0.10(3.91 \pm 0.22), & G_{D^-(2S)\bar{D}^{*0}\pi^-} &= 5.27 \pm 0.22(5.69 \pm 0.60), \\
G_{D^-(2S)D_0^{*-}\pi^0} &= 0.70 \pm 0.12(0.40 \pm 0.10) \text{ GeV}, & G_{D^-(2S)\bar{D}_0^{*0}\pi^-} &= 0.92 \pm 0.35(0.63 \pm 0.22) \text{ GeV}, \\
G_{D_s^-(2S)\bar{D}^{*0}K^-} &= 7.76 \pm 0.65(6.76 \pm 0.50), & G_{D_s^-(2S)D^{*-}\bar{K}^0} &= 7.77 \pm 0.60(6.68 \pm 0.47), \\
G_{B^+(2S)B^{*+}\pi^0} &= 9.93 \pm 0.25(11.02 \pm 0.31), & G_{B^+(2S)B^{*0}\pi^+} &= 14.04 \pm 0.33(15.51 \pm 0.62), \\
G_{B^+(2S)B_0^{*+}\pi^0} &= 1.32 \pm 0.10(1.62 \pm 0.12) \text{ GeV}, & G_{B^+(2S)B_0^{*0}\pi^+} &= 2.01 \pm 0.25(2.22 \pm 0.30) \text{ GeV}, \\
G_{B^0(2S)B^{*0}\pi^0} &= 9.89 \pm 0.30(11.02 \pm 0.39), & G_{B^0(2S)B^{*+}\pi^-} &= 14.07 \pm 0.34(15.72 \pm 0.56), \\
G_{B^0(2S)B_0^{*0}\pi^0} &= 1.33 \pm 0.11(1.62 \pm 0.12) \text{ GeV}, & G_{B^0(2S)B_0^{*+}\pi^-} &= 1.88 \pm 0.22(2.34 \pm 0.25) \text{ GeV}, \\
G_{B_s(2S)B^{*+}K^-} &= 20.09 \pm 0.44(17.81 \pm 0.68), & G_{B_s(2S)B^{*0}\bar{K}^0} &= 20.22 \pm 0.28(17.36 \pm 0.42). \quad (11)
\end{aligned}$$

Tables IV and V show the strong decay widths. Comparing equation (11) with table IV, we find that the uncertainties of strong decay widths are very large, even if there are small uncertainties of strong coupling constants. This indicates that the predicted decay widths are very sensitive to the mass (or kinematic range). The two methods adopted in this paper, i.e. the low-energy approximation and the the impulse approximation, obtained similar strong decay widths, except some of the channels with  $P$ -wave involved, which have large discrepancies. As one can see, these  $P$ -wave-involved channels have much smaller phase spaces than other channels, which show that these two methods give different results in small phase space. And we pointed out one more time that the large uncertainties in table IV and V show that the decay widths are very sensitive to the node structures of  $2S$  states.

We find that there are two dominant OZI-allowed decay channels for all the heavy-light  $2S$  states in table IV, both of which are the case of  $0^-(2S) \rightarrow 1^-0^-$ . Other available OZI-allowed strong decay channels ( $0^-(2S) \rightarrow 0^+0^-, 2^+0^-$ ) include heavy  $P$ -wave meson ( $0^+$  or  $2^+$ ) in the final states, e.g.,  $\bar{D}^0(2S) \rightarrow \bar{D}_0^*(2400)^0\pi^0$ , where  $D_0^*(2400)^0$  is a scalar ( $0^+$ ) meson. Compared with the decays whose final states are all  $S$ -wave meson ( $1^-$  and  $0^-$ ), that includes  $P$ -wave meson in the final state and has a small decay width. In table IV we do not show the channels

TABLE IV: The decay widths (in unit of MeV) of strong decay modes.  $\Gamma_1$  and  $\Gamma_2$  come from the impulse approximation and the low-energy approximation, respectively.

Modes	$\Gamma_1$	$\Gamma_2$	Modes	$\Gamma_1$	$\Gamma_2$
$\bar{D}^0(2S) \rightarrow \bar{D}^{*0}\pi^0$	$15.2 \pm 6.9$	$14.1 \pm 7.5$	$\bar{D}^0(2S) \rightarrow D^{*-}\pi^+$	$31 \pm 10$	$27 \pm 15$
$\bar{D}^0(2S) \rightarrow \bar{D}_0^*(2400)^0\pi^0$	$0.182 \pm 0.058$	$0.83 \pm 0.30$	$\bar{D}^0(2S) \rightarrow D_0^*(2400)^-\pi^+$	$0.35 \pm 0.20$	$1.39 \pm 0.57$
$D^-(2S) \rightarrow D^{*-}\pi^0$	$16.4 \pm 6.6$	$14.5 \pm 7.5$	$D^-(2S) \rightarrow \bar{D}^{*0}\pi^-$	$33 \pm 10$	$30 \pm 15$
$D^-(2S) \rightarrow D_0^*(2400)^-\pi^0$	$0.21 \pm 0.10$	$0.62 \pm 0.30$	$D^-(2S) \rightarrow \bar{D}_0^*(2400)^0\pi^-$	$0.52 \pm 0.32$	$1.10 \pm 0.62$
$D_s^-(2S) \rightarrow \bar{D}^{*0}K^-$	$19 \pm 20$	$25 \pm 26$	$D_s^-(2S) \rightarrow D^{*-}\bar{K}^0$	$17 \pm 18$	$24 \pm 25$
$B^+(2S) \rightarrow B^{*+}\pi^0$	$30.1 \pm 4.0$	$24.1 \pm 6.0$	$B^+(2S) \rightarrow B^{*0}\pi^+$	$59 \pm 13$	$48 \pm 12$
$B^+(2S) \rightarrow B_0^{*+}\pi^0$	$0.85 \pm 0.25$	$0.45 \pm 0.15$	$B^+(2S) \rightarrow B_0^{*0}\pi^+$	$1.61 \pm 0.41$	$1.04 \pm 0.31$
$B^0(2S) \rightarrow B^{*0}\pi^0$	$30.1 \pm 4.8$	$24.0 \pm 4.4$	$B^0(2S) \rightarrow B^{*+}\pi^-$	$60 \pm 13$	$48 \pm 12$
$B^0(2S) \rightarrow B_0^{*0}\pi^0$	$0.85 \pm 0.24$	$0.46 \pm 0.15$	$B^0(2S) \rightarrow B_0^{*+}\pi^-$	$1.81 \pm 0.50$	$0.91 \pm 0.31$
$B_s(2S) \rightarrow B^{*+}K^-$	$42 \pm 18$	$55 \pm 19$	$B_s(2S) \rightarrow B^{*0}\bar{K}^0$	$41 \pm 18$	$54 \pm 19$

that involve heavy tensor meson ( $J^P = 2^+$ ), which has an ignorable decay width caused by the extremely narrow kinematic range. There are not enough experimental data for the scalars mesons ( $J^P = 0^+$ ). For example,  $\bar{D}_0^*(2400)^0$  has been confirmed, but  $D_0^*(2400)^-$  is missing. So we choose the same mass for  $\bar{D}_0^{*0}$  and  $D_0^{*-}$ , i.e.  $M_{\bar{D}_0^*(2400)^0} = 2.296 \pm 0.095$  GeV, and the same mass for  $B_0^{*0}$  and  $B_0^{*+}$ , i.e.  $M_{B_0^{*0}} = 5.660 \pm 0.266$  GeV. For the decays of  $D_s(2S)$  and  $B_s(2S)$ , the channels involving  $P$ -wave state in the final states are kinematic forbidden.

Since we have obtained higher masses for heavy-light  $2S$  states than the ones of the previous letter [23], we obtain much broader widths, but the estimated full width of  $\bar{D}^0(2S)$  is still narrower than the experimental data of  $D(2550)^0$ . Our prediction is  $\Gamma_{\bar{D}^0(2S)} = 47 \pm 17(43 \pm 23)$  MeV, while from data is  $130 \pm 12 \pm 13$  MeV [9]. The new state  $D(2550)^0$  should be the state  $D^0(2S)$  around the 2540 MeV, since other states can be ruled out by the masses or decay modes. For example,  $P$ -wave  $D_{sJ}^*$  states whose masses are closed to 2540 MeV have strong decay productions including  $K$  or  $D_s$  but not  $D^*\pi$ . The  $P$ -wave  $D_J^*$  states, which have masses about 100 MeV lower than 2540 MeV, have strong decays different from  $0^-(2S)$ . For  $D$ -mesons, which are  $1^-(2S)$ ,  $1^-(2D)$ , or the mixing of  $1^-(2S)$  and  $1^-(2D)$ , their masses should be higher than 2540 MeV and we already have the candidate

TABLE V: The estimated full widths (in unit of MeV) of the first radial excited states. The first and second value (in brackets) come from low-energy approximation and impulse approximation, respectively.

$\bar{D}^0(2S)$	$D^-(2S)$	$D_s^-(2S)$	$B^0(2S)$	$B^+(2S)$	$B_s(2S)$
$43 \pm 23(47 \pm 17)$	$46 \pm 23(50 \pm 17)$	$49 \pm 51(36 \pm 38)$	$74 \pm 17(91 \pm 18)$	$73 \pm 19(93 \pm 19)$	$109 \pm 38(83 \pm 36)$

$D^*(2600)$  [9] that have more strong decay channels:  $0^-1^-$ ,  $0^-0^-$ ,  $1^-1^-$ ,  $1^-0^+$ . Therefore, the new state  $D(2550)^0$  is the state  $D^0(2S)$ . The discrepancy between the theoretical and experimental result comes from that we only considered the dominant OZI-allowed strong decays. Finally, we should point out that the experimental data may vary along with new more precise detections.

### C. Product of semi-leptonic decay ratio and cascaded strong decay ratio

We have calculated  $B_{q'}$  semi-leptonic decay to  $B_q(2S)$  and  $D_q(2S)$ , where all the states are on mass shells; we also calculated the main strong decays of  $B_q(2S)$  and  $D_q(2S)$ , e.g., we obtain the branching ratio of the semi-leptonic decay  $Br(B^+ \rightarrow \bar{D}^0(2S)\ell^+\nu_\ell) = (5.1 \pm 1.5) \times 10^{-4}$ , the strong decay branching ratio  $Br(\bar{D}^0(2S) \rightarrow D^{*-}\pi^+) = \frac{\Gamma_{\bar{D}^0(2S) \rightarrow D^{*-}\pi^+}}{\Gamma_{\bar{D}^0(2S)}} = 0.63 \pm 0.48(0.66 \pm 0.15)$  and  $Br(\bar{D}^0(2S) \rightarrow \bar{D}^{*0}\pi^0) = \frac{\Gamma_{\bar{D}^0(2S) \rightarrow \bar{D}^{*0}\pi^0}}{\Gamma_{\bar{D}^0(2S)}} = 0.33 \pm 0.24(0.32 \pm 0.11)$ . To reduce the influence of the discrepancies caused by the theoretical strong decay widths, and the ground  $1S$  states  $D^{(*)}$ ,  $B^{(*)}$ , and their decays that are well known in the experiment, we multiply the branching ratio of the semi-leptonic decay with the strong decay branching ratio, which show the ability of experiment to detect the missing  $2S$  states, but we ignore the reconstructed efficiencies of events in experiment, and the products of ratios are

$$Br(B^+ \rightarrow \bar{D}^0(2S)\ell^+\nu_\ell) \times Br(\bar{D}^0(2S) \rightarrow D^{*-}\pi^+) \approx [3.2 \pm 2.6(3.4 \pm 1.9)] \times 10^{-4},$$

$$Br(B^+ \rightarrow \bar{D}^0(2S)\ell^+\nu_\ell) \times Br(\bar{D}^0(2S) \rightarrow \bar{D}^{*0}\pi^0) \approx [1.7 \pm 1.4(1.6 \pm 1.0)] \times 10^{-4}, \quad (12)$$

$$Br(B^0 \rightarrow D^-(2S)\ell^+\nu_\ell) \times Br(D^-(2S) \rightarrow \bar{D}^{*0}\pi^-) \approx [3.0 \pm 2.3(3.0 \pm 1.6)] \times 10^{-4},$$

$$Br(B^0 \rightarrow D^-(2S)\ell^+\nu_\ell) \times Br(D^-(2S) \rightarrow D^{*-}\pi^0) \approx [1.4 \pm 1.1(1.5 \pm 0.9)] \times 10^{-4}, \quad (13)$$

$$Br(B_s^0 \rightarrow D_s^-(2S)\ell^+\nu_\ell) \times Br(D_s^-(2S) \rightarrow \bar{D}^{*0}K^-) \approx [5.1 \pm 7.6(5.2 \pm 7.9)] \times 10^{-4},$$

$$Br(B_s^0 \rightarrow D_s^-(2S)\ell^+\nu_\ell) \times Br(D_s^-(2S) \rightarrow D^{*-}\bar{K}^0) \approx [4.8 \pm 7.3(4.7 \pm 7.1)] \times 10^{-4}, \quad (14)$$

$$\begin{aligned}
Br(B_c^+ \rightarrow B^0(2S)\ell^+\nu_\ell) \times Br(B^0(2S) \rightarrow B^{*+}\pi^-) &\approx [0.79 \pm 0.47(0.79 \pm 0.46)] \times 10^{-6}, \\
Br(B_c^+ \rightarrow B^0(2S)\ell^+\nu_\ell) \times Br(B^0(2S) \rightarrow B^{*0}\pi^0) &\approx [0.39 \pm 0.23(0.40 \pm 0.22)] \times 10^{-6}, \quad (15)
\end{aligned}$$

$$\begin{aligned}
Br(B_c^+ \rightarrow B_s^0(2S)\ell^+\nu_\ell) \times Br(B_s(2S) \rightarrow B^{*+}K^-) &\approx [1.9 \pm 1.5(1.9 \pm 1.4)] \times 10^{-6}, \\
Br(B_c^+ \rightarrow B_s^0(2S)\ell^+\nu_\ell) \times Br(B_s(2S) \rightarrow B^{*0}\bar{K}^0) &\approx [1.8 \pm 1.5(1.8 \pm 1.4)] \times 10^{-6}. \quad (16)
\end{aligned}$$

The decays of  $B^+$  and  $B^0$  have ratios of order  $10^{-4}$ , which can be analyzed with current data at B-factories. The decay of  $B_s$  that has ratios of order  $10^{-4}$  may be observed in the future, while the  $B_c$  decay ratio of order  $10^{-6}$  is hard to reach experimentally.

In summary, we have studied the productions of  $D_q(2S)$  and  $B_q(2S)$  in the exclusive semi-leptonic  $B_{q'}$  decays and the strong decays of  $D_q(2S)$  and  $B_q(2S)$ . Some of these decays have the branching ratios of order  $10^{-4}$ , which could be measured currently in experiments. For examples, the ratios  $Br(B^+ \rightarrow \bar{D}^0(2S)\ell^+\nu_\ell) \times Br(\bar{D}^0(2S) \rightarrow \bar{D}^*\pi) \approx [4.9 \pm 4.0(5.0 \pm 2.9)] \times 10^{-4}$  and  $Br(B^0 \rightarrow D^-(2S)\ell^+\nu_\ell) \times Br(D^-(2S) \rightarrow \bar{D}^*\pi) \approx [4.4 \pm 3.4(4.5 \pm 2.5)] \times 10^{-4}$  are relatively large in  $B$  decays, which could be detected by the two current  $B$ -factories. For  $D_s(2S)$ , the ratio  $Br(B_s^0 \rightarrow D_s^-(2S)\ell^+\nu_\ell) \times Br(D_s^-(2S) \rightarrow \bar{D}^*\bar{K}) \approx [9.9 \pm 14.9(9.9 \pm 15.0)] \times 10^{-4}$  is also not small, which will be reached in the future. We have also given the strong coupling constants of  $D_q(2S)$  and  $B_q(2S)$ , which maybe observed experimentally. Although similar to other models' results, our calculation also gave a smaller full decay width than the experimental data, but the recent detected  $D(2550)^0$  is very likely the  $D^0(2S)$  state.

**Acknowledgements** This work was supported in part by the National Natural Science Foundation of China (NSFC) under Grant numbers 10875032 and 11175051.

## Appendix A: Instantaneous BS Equation

In this section, we briefly review the BS equation and its instantaneous one, i.e., the Salpeter equation.

The BS equation is read as [43]

$$(\not{p}_1 - m_1)\chi(q)(\not{p}_2 + m_2) = i \int \frac{d^4k}{(2\pi)^4} V(P, k, q)\chi(k), \quad (A1)$$

where  $\chi(q)$  is the BS wavefunction,  $V(P, k, q)$  is the interaction kernel between the quark and anti-quark, and  $p_1$  and  $p_2$  are the momenta of the quark 1 and anti-quark 2.

We divide the relative momentum  $q$  into two parts, i.e.,  $q_{\parallel}$  and  $q_{\perp}$ :

$$q^\mu = q_{\parallel}^\mu + q_{\perp}^\mu,$$

$$q_{\parallel}^{\mu} \equiv (P \cdot q/M^2)P^{\mu} , \quad q_{\perp}^{\mu} \equiv q^{\mu} - q_{\parallel}^{\mu} .$$

In the instantaneous approach, the kernel  $V(P, k, q)$  takes the simple form[44]:

$$V(P, k, q) \Rightarrow V(|\vec{k} - \vec{q}|) .$$

Let us introduce the notations  $\varphi_p(q_{\perp}^{\mu})$  and  $\eta(q_{\perp}^{\mu})$  for a three-dimensional wavefunction as follows:

$$\begin{aligned} \varphi_p(q_{\perp}^{\mu}) &\equiv i \int \frac{dq_p}{2\pi} \chi(q_{\parallel}^{\mu}, q_{\perp}^{\mu}) , \\ \eta(q_{\perp}^{\mu}) &\equiv \int \frac{dk_{\perp}}{(2\pi)^3} V(k_{\perp}, q_{\perp}) \varphi_p(k_{\perp}^{\mu}) . \end{aligned} \quad (\text{A2})$$

Then, the BS equation can be rewritten as

$$\chi(q_{\parallel}, q_{\perp}) = S_1(p_1) \eta(q_{\perp}) S_2(p_2) . \quad (\text{A3})$$

The propagators of the two constituents can be decomposed as:

$$S_i(p_i) = \frac{\Lambda_{ip}^+(q_{\perp})}{J(i)q_p + \alpha_i M - \omega_i + i\epsilon} + \frac{\Lambda_{ip}^-(q_{\perp})}{J(i)q_p + \alpha_i M + \omega_i - i\epsilon} , \quad (\text{A4})$$

with

$$\omega_i = \sqrt{m_i^2 + q_T^2} , \quad \Lambda_{ip}^{\pm}(q_{\perp}) = \frac{1}{2\omega_{ip}} \left[ \frac{P}{M} \omega_i \pm J(i)(m_i + \not{q}_{\perp}) \right] , \quad (\text{A5})$$

where  $i = 1, 2$  for quark and anti-quark, respectively, and  $J(i) = (-1)^{i+1}$ .

We introduce the notations  $\varphi_p^{\pm\pm}(q_{\perp})$  as

$$\varphi_p^{\pm\pm}(q_{\perp}) \equiv \Lambda_{1p}^{\pm}(q_{\perp}) \frac{P}{M} \varphi_p(q_{\perp}) \frac{P}{M} \Lambda_{2p}^{\pm}(q_{\perp}) . \quad (\text{A6})$$

With contour integration over  $q_p$  on both sides of equation (A3), we obtain

$$\varphi_p(q_{\perp}) = \frac{\Lambda_{1p}^+(q_{\perp}) \eta_p(q_{\perp}) \Lambda_{2p}^+(q_{\perp})}{(M - \omega_1 - \omega_2)} - \frac{\Lambda_{1p}^-(q_{\perp}) \eta_p(q_{\perp}) \Lambda_{2p}^-(q_{\perp})}{(M + \omega_1 + \omega_2)} ,$$

and the full Salpeter equation

$$\begin{aligned} (M - \omega_1 - \omega_2) \varphi_p^{++}(q_{\perp}) &= \Lambda_{1p}^+(q_{\perp}) \eta_p(q_{\perp}) \Lambda_{2p}^+(q_{\perp}) , \\ (M + \omega_1 + \omega_2) \varphi_p^{--}(q_{\perp}) &= -\Lambda_{1p}^-(q_{\perp}) \eta_p(q_{\perp}) \Lambda_{2p}^-(q_{\perp}) , \\ \varphi_p^{+-}(q_{\perp}) &= \varphi_p^{-+}(q_{\perp}) = 0 . \end{aligned} \quad (\text{A7})$$

For the different  $J^{PC}$  (or  $J^P$ ) states, we give the general form of wavefunctions (we will talk about them in appendix B). Reduce the wavefunctions by the last equation of (A7),



and then solve the first and second equations of (A7) to obtain the wavefunctions and mass spectrum. We have discussed the solution of the Salpeter equation in detail in [21, 29].

The normalization condition for the BS wavefunction is

$$\int \frac{q_T^2 dq_T}{2\pi^2} Tr \left[ \bar{\varphi}^{++} \frac{P}{M} \varphi^{++} \frac{P}{M} - \bar{\varphi}^{--} \frac{P}{M} \varphi^{--} \frac{P}{M} \right] = 2P_0. \quad (\text{A8})$$

In our model, the instantaneous interaction kernel  $V$  is the Cornell potential, which is the sum of a linear scalar interaction and a vector interaction:

$$V(r) = V_s(r) + V_0 + \gamma_0 \otimes \gamma^0 V_v(r) = \lambda r + V_0 - \gamma_0 \otimes \gamma^0 \frac{4\alpha_s}{3r}, \quad (\text{A9})$$

where  $\lambda$  is the string constant and  $\alpha_s(\vec{q})$  is the running coupling constant. In order to fit the data of heavy quarkonia, a constant  $V_0$  is often added to the confine potential. One can see that  $V_v(r)$  diverges at  $r = 0$ ; we introduce a factor  $e^{-\alpha r}$  to avoid the divergence

$$V_s(r) = \frac{\lambda}{\alpha}(1 - e^{-\alpha r}), \quad V_v(r) = -\frac{4\alpha_s}{3r} e^{-\alpha r}. \quad (\text{A10})$$

It is easy to know that when  $\alpha r \ll 1$ , the potential becomes equation (A9). In the momentum space and the center of mass system of the bound state, the potential reads :

$$V(\vec{q}) = V_s(\vec{q}) + \gamma_0 \otimes \gamma^0 V_v(\vec{q}),$$

$$V_s(\vec{q}) = -\left(\frac{\lambda}{\alpha} + V_0\right)\delta^3(\vec{q}) + \frac{\lambda}{\pi^2} \frac{1}{(\vec{q}^2 + \alpha^2)^2}, \quad V_v(\vec{q}) = -\frac{2}{3\pi^2} \frac{\alpha_s(\vec{q})}{(\vec{q}^2 + \alpha^2)}, \quad (\text{A11})$$

where the running coupling constant  $\alpha_s(\vec{q})$  is

$$\alpha_s(\vec{q}) = \frac{12\pi}{33 - 2N_f} \frac{1}{\log\left(a + \frac{\vec{q}^2}{\Lambda_{QCD}^2}\right)}.$$

We introduce a small parameter  $a$  to avoid the divergence in the denominator. The constants  $\lambda$ ,  $\alpha$ ,  $V_0$  and  $\Lambda_{QCD}$  are the parameters that characterize the potential.  $N_f = 3$  for  $\bar{b}q$  (and  $\bar{c}q$ ) system.

## Appendix B: Wavefunctions for different states

We know that form factors of semi-leptonic decay and strong coupling constants of strong decay are related to wavefunctions of different states in section II and III. In this section, we give the wavefunctions of the different states and obtain the form factors and strong coupling constants.

**a). For  $B_{q'}$  meson with quantum numbers  $J^P = 0^-$**

The general form for the relativistic wavefunction of pseudoscalar meson can be written as [29]

$$\varphi_{0^-}(\vec{q}) = \left[ f_1(\vec{q})\mathcal{P} + f_2(\vec{q})M + f_3(\vec{q})\not{q}_\perp + f_4(\vec{q})\frac{\mathcal{P}\not{q}_\perp}{M} \right] \gamma_5, \quad (\text{B1})$$

where  $M$  is the mass of the pseudoscalar meson, and  $f_i(\vec{q})$  are functions of  $|\vec{q}|^2$ . Due to the last two equations of (A7):  $\varphi_{0^-}^{+-} = \varphi_{0^-}^{-+} = 0$ , we have

$$f_3(\vec{q}) = \frac{f_2(\vec{q})M(-\omega_1 + \omega_2)}{m_2\omega_1 + m_1\omega_2}, \quad f_4(\vec{q}) = -\frac{f_1(\vec{q})M(\omega_1 + \omega_2)}{m_2\omega_1 + m_1\omega_2}. \quad (\text{B2})$$

where  $m_1$  and  $m_2$  and  $\omega_1 = \sqrt{m_1^2 + \vec{q}^2}$ ,  $\omega_2 = \sqrt{m_2^2 + \vec{q}^2}$  are the masses and the energies of quark and anti-quark in  $B_{q'}$  mesons,  $q_\perp = q - (q \cdot P/M^2)P$ , and  $q_\perp^2 = -|\vec{q}|^2$ . Then, there are only two independent unknown wavefunctions  $f_1(\vec{q})$  and  $f_2(\vec{q})$  in equation (B1):

$$\begin{aligned} \varphi_{0^-}(\vec{q}) = & \left[ f_1(\vec{q})\mathcal{P} + f_2(\vec{q})M - f_2(\vec{q})\not{q}_\perp \frac{M(\omega_1 - \omega_2)}{m_2\omega_1 + m_1\omega_2} \right. \\ & \left. + f_1(\vec{q})\not{q}_\perp \mathcal{P} \frac{\omega_1 + \omega_2}{m_2\omega_1 + m_1\omega_2} \right] \gamma_5. \end{aligned} \quad (\text{B3})$$

The numerical values of radial wavefunctions  $f_1$  and  $f_2$  and eigenvalue  $M$  can be obtained by solving the first two Salpeter equations in equation (A7).

According to equation (A6), the relativistic positive wavefunction of pseudoscalar  $0^-$  state in center of mass system can be written as [29]

$$\varphi_{0^-}^{++}(\vec{q}) = b_1 \left[ b_2 + \frac{\mathcal{P}}{M} + b_3 \not{q}_\perp + b_4 \frac{\not{q}_\perp \mathcal{P}}{M} \right] \gamma_5, \quad (\text{B4})$$

where the  $b_i$ s ( $i = 1, 2, 3, 4$ ) are related to the original radial wavefunction  $f_i$ , quark masses  $m_i$ , quark energy  $w_i$  ( $i = 1, 2$ ) and meson mass  $M$ :

$$b_1 = \frac{M}{2} \left( f_1(\vec{q}) + f_2(\vec{q}) \frac{m_1 + m_2}{\omega_1 + \omega_2} \right), b_2 = \frac{\omega_1 + \omega_2}{m_1 + m_2}, b_3 = -\frac{(m_1 - m_2)}{m_1\omega_2 + m_2\omega_1}, b_4 = \frac{(\omega_1 + \omega_2)}{(m_1\omega_2 + m_2\omega_1)}.$$

**b). For  $B_q(2S)$  and  $D_q(2S)$  mesons with quantum numbers  $J^P = 0^-$**

Because the  $2S$  state mesons have the same quantum numbers as  $B_{q'}$ , the wavefunction of  $2S$  state mesons are similar to equation (B4),

$$\varphi_{P_f}^{++}(\vec{q}_f) = a_1 \left[ a_2 + \frac{\mathcal{P}_f}{M_f} + a_3 \not{q}_{f\perp} + a_4 \frac{\not{q}_{f\perp} \mathcal{P}_f}{M_f} \right] \gamma_5, \quad (\text{B5})$$

$$a_1 = \frac{M_f}{2} \left( f'_1(\vec{q}_f) + f'_2(\vec{q}_f) \frac{m'_1 + m'_2}{\omega'_1 + \omega'_2} \right), a_2 = \frac{\omega'_1 + \omega'_2}{m'_1 + m'_2}, a_3 = -\frac{(m'_1 - m'_2)}{m'_1\omega'_2 + m'_2\omega'_1}, a_4 = \frac{(\omega'_1 + \omega'_2)}{(m'_1\omega'_2 + m'_2\omega'_1)}.$$

where  $M_f$ ,  $P_f$  and  $f'_i(\vec{q}_f)$  are the mass, momentum and the radial wavefunction of  $2S$  state mesons, respectively.  $m'_1, m'_2$  and  $\omega'_1 = \sqrt{m'^2_1 + \vec{q}^2_f}, \omega'_2 = \sqrt{m'^2_2 + \vec{q}^2_f}$  are the masses and the energies of quark and anti-quark in  $2S$  state mesons, respectively.

According to the equations (9), (B4) and (B5), the form factors of  $B_{q'}$  semi-leptonic decays to  $2S$  state mesons can be written as

$$f_+ = \frac{1}{2} \int \frac{d^3q}{(2\pi)^3} \frac{4a_1b_1}{MM_f} \left[ (a_2b_2M_f + b_3q \cdot r \cos \theta - a_4b_2E_f^2\alpha'_1 - a_4b_4E_fq \cdot r \cos \theta)\alpha'_1 \right. \\ \left. + a_3M_f(b_3q^2 + E_f\alpha'_1 - b_3q \cdot r \cos \theta\alpha'_1) + M(1 + a_4b_4q^2 + a_4b_2E_f\alpha'_1 - a_3M_f\alpha'_1) \right. \\ \left. - M(1 - \frac{E_f}{M})(a_4b_2E_f - b_3E_f - a_3M_f + a_2b_4M_f + a_4b_4q \cdot r \cos \theta) \right], \quad (\text{B6})$$

$$f_- = \frac{1}{2} \int \frac{d^3q}{(2\pi)^3} \frac{4a_1b_1}{MM_f} \left[ (a_2b_2M_f + b_3q \cdot r \cos \theta - a_4b_2E_f^2\alpha'_1 - a_4b_4E_fq \cdot r \cos \theta)\alpha'_1 \right. \\ \left. + a_3M_f(b_3q^2 + E_f\alpha'_1 - b_3q \cdot r \cos \theta\alpha'_1) - M(1 + a_4b_4q^2 + a_4b_2E_f\alpha'_1 - a_3M_f\alpha'_1) \right. \\ \left. + M(1 + \frac{E_f}{M})(a_4b_2E_f - b_3E_f - a_3M_f + a_2b_4M_f + a_4b_4q \cdot r \cos \theta) \right], \quad (\text{B7})$$

where  $E_f = \sqrt{M_f^2 + \vec{r}^2}$ ,  $q \cdot r \equiv |\vec{q} \cdot \vec{r}|$ ,  $\theta$  is the angle between  $\vec{q}$  and  $\vec{r}$ .

**c). For  $B_q^*$  and  $D_q^*$  mesons with quantum numbers  $J^P = 1^-$**

The relativistic positive wavefunction of  $1^-$  state can be written as

$$\varphi_{1^-}^{++}(\vec{q}_{f1}) = c_1 \not{\epsilon}^{(\lambda)} + c_2 \not{\epsilon}^{(\lambda)} \not{P}_{f1} + c_3 (\not{q}_{f1\perp} \not{\epsilon}^{(\lambda)} - q_{f1\perp} \cdot \epsilon^{(\lambda)}) + c_4 (\not{P}_{f1} \not{\epsilon}^{(\lambda)} \not{q}_{f1\perp} - \not{P}_{f1} q_{f1\perp} \cdot \epsilon^{(\lambda)}) \\ + q_{f1\perp} \cdot \epsilon^{(\lambda)} (c_5 + c_6 \not{P}_{f1} + c_7 \not{q}_{f1\perp} + c_8 \not{q}_{f1\perp} \not{P}_{f1}), \quad (\text{B8})$$

where we first defined the parameter  $n_i$  that is functions of  $f''_i$  ( $1^-$  wave functions):

$$n_1 = f''_5(\vec{q}_{f1}) - f''_6(\vec{q}_{f1}) \frac{(\omega''_1 + \omega''_2)}{(m''_1 + m''_2)}, n_2 = f''_5(\vec{q}_{f1}) - f''_6(\vec{q}_{f1}) \frac{(m''_1 + m''_2)}{(\omega''_1 + \omega''_2)}, \\ n_3 = f''_3(\vec{q}_{f1}) + f''_4(\vec{q}_{f1}) \frac{(m''_1 + m''_2)}{(\omega''_1 + \omega''_2)}.$$

Then, we defined the parameters  $c_i$  that are functions of  $f''_i$  and  $n_i$ :

$$c_1 = \frac{M_{f1}}{2} n_1, c_2 = -\frac{1}{2} \frac{(m''_1 + m''_2)}{(\omega''_1 + \omega''_2)} n_1, c_3 = \frac{M_{f1}}{2} \frac{(\omega''_2 - \omega''_1)}{(m''_1\omega''_2 + m''_2\omega''_1)} n_1, c_4 = \frac{1}{2} \frac{(\omega''_1 + \omega''_2)}{(\omega''_1\omega''_2 + m''_1m''_2 - q_{f1\perp}^2)} n_1, \\ c_5 = \frac{1}{2M_{f1}} \frac{m''_1 + m''_2}{(\omega''_1\omega''_2 + m''_1m''_2 + q_{f1\perp}^2)} (M_{f1}^2 n_2 + q_{f1\perp}^2 n_3), c_6 = \frac{1}{2M_{f1}} \frac{\omega''_1 - \omega''_2}{(\omega''_1\omega''_2 + m''_1m''_2 + q_{f1\perp}^2)} (M_{f1}^2 n_2 + q_{f1\perp}^2 n_3), \\ c_7 = \frac{n_3}{2M_{f1}} - \frac{f''_6(\vec{q}_{f1})M_{f1}}{(m''_1\omega''_2 + m''_2\omega''_1)}, c_8 = \frac{1}{2M_{f1}} \frac{\omega''_1 + \omega''_2}{m''_1 + m''_2} n_3 - f''_5(\vec{q}_{f1}) \frac{\omega''_1 + \omega''_2}{(m''_1 + m''_2)(\omega''_1\omega''_2 + m''_1m''_2 - q_{f1\perp}^2)}.$$

According to equations (10), (B5) and (B8), the strong coupling constant for  $0^-(2S) \rightarrow 1^-0^-$  can be written as

$$\begin{aligned}
G_{0^-(2S) \rightarrow 1^-0^-} = & \frac{1}{f_X} \int \frac{d^3q_f}{(2\pi)^3} 4a_1 \left\{ \frac{1}{M_f} \left[ (a_4c_3M_f + a_3c_4M_{f1}^2)|\vec{q}_f|^2 - a_4c_2M_f\vec{q}_f \cdot \vec{P}_{f1} \right. \right. \\
& + a_3c_4(\vec{q}_f \cdot \vec{P}_{f1})^2 - c_1(M_f + a_3\vec{q}_f \cdot \vec{P}_{f1}) + c_6E_{f1}\alpha_2''(E_{f1}M_f - M_{f1}^2) + a_3c_7|\vec{q}_f|^2E_{f1}\alpha_2''(M_f - E_{f1}) \\
& a_4c_8|\vec{q}_f|^2E_{f1}\alpha_2''(E_{f1}M_f - M_{f1}^2) + (c_7E_{f1} - a_4c_5E_{f1} + a_3c_4E_{f1}^2 + a_4c_3M_f + a_3c_6E_{f1}M_f)\vec{q}_f \cdot \vec{P}_{f1}\alpha_2'' \\
& - a_4c_8E_{f1}\alpha_2''(\vec{q}_f \cdot \vec{P}_{f1})^2 + c_7E_{f1}\alpha_2''|\vec{P}_{f1}|^2 + a_3c_7\vec{q}_f \cdot \vec{P}_{f1}\alpha_2''E_{f1}(M_f - E_{f1}) \\
& + a_4c_8E_{f1}^2\alpha_2''(M_f - E_{f1}) + a_2(c_2M_{f1}^2 + c_3(\vec{q}_f \cdot \vec{P}_{f1} + |\vec{P}_{f1}|^2)\alpha_2'') \\
& + E_{f1}\alpha_2''(c_5(E_{f1} - M_f) + c_8E_{f1}(\vec{q}_f \cdot \vec{P}_{f1} + E_{f1}^2\alpha_2'' - M_{f1}^2\alpha_2'')) \left. \right] - \frac{E_{f1}|\vec{q}_f|}{M_f|\vec{P}_{f1}|} [a_2c_5(M_f - E_{f1}) \\
& + (a_4c_2 + c_6)(M_{f1}^2 - E_{f1}M_f) + a_4c_8|\vec{q}_f|^2(M_{f1}^2 - E_{f1}M_f) + (a_4c_3 + a_4c_5 - c_7 - a_2c_8E_{f1})\vec{q}_f \cdot \vec{P}_{f1} \\
& + a_4c_8|\vec{q}_f \cdot \vec{P}_{f1}|^2 + (a_4c_3 - c_7)E_{f1}^2\alpha_2'' - a_2c_8E_{f1}^3\alpha_2'' + (c_7 - a_4c_3)M_{f1}^2\alpha_2'' + a_2c_8E_{f1}M_{f1}^2\alpha_2'' \\
& + a_4c_8\vec{q}_f \cdot \vec{P}_{f1}\alpha_2''E_{f1}(E_{f1} - M_{f1}) + a_3(c_1(M_f - E_{f1}) + (c_4E_{f1} - c_6M_f)\vec{q}_f \cdot \vec{P}_{f1} \\
& + c_4E_{f1}\alpha_2''|\vec{P}_{f1}|^2 + c_7(E_{f1} - M_f)(|\vec{q}_f|^2 + \vec{q}_f \cdot \vec{P}_{f1}\alpha_2'')) \left. \right\} \quad (B9)
\end{aligned}$$

where  $f_X$  ( $X$  is  $\pi$  or  $K$ ) is the decay constant for the light meson,  $\alpha_2'' = \frac{m_2''}{m_1'' + m_2''}$ .

**d). For  $B_q^*$  and  $D_q^*$  mesons with quantum numbers  $J^P = 0^+$**

The relativistic positive energy wavefunction of  $0^+$  can be written as

$$\varphi_{0^+}^{++}(\vec{q}_{f1}) = c_1(\not{q}_{f1\perp} + c_2\frac{\not{P}_{f1}\not{q}_{f1\perp}}{M_{f1}} + c_3 + c_4\frac{\not{P}_{f1}}{M_{f1}}), \quad (B10)$$

where the parameters  $c_i$  are the functions of  $f_1''$  and  $f_2''$  ( $0^+$  wavefunction), which are defined as

$$c_1 = \frac{1}{2} \left( f_1''(\vec{q}_{f1}) + f_2''(\vec{q}_{f1}) \frac{m_1'' + m_2''}{\omega_1'' + \omega_2''} \right), c_2 = \frac{\omega_1'' + \omega_2''}{m_1'' + m_2''}, c_3 = q_{f1\perp}^2 \frac{(\omega_1'' + \omega_2'')}{m_1''\omega_2'' + m_2''\omega_1''}, c_4 = \frac{(m_2''\omega_1'' - m_1''\omega_2'')}{(m_1'' + m_2'')}.$$

Using equations (10), (B5) and (B10), the strong coupling constant for  $0^-(2S) \rightarrow 0^+0^-$  can be written as

$$\begin{aligned}
G_{0^-(2S) \rightarrow 0^+0^-} = & \frac{1}{f_X} \int \frac{d^3q_f}{(2\pi)^3} \frac{-4a_1c_1}{M_{f1}} \left\{ (a_4c_2E_{f1}M_f - a_3E_{f1}M_{f1} + a_3M_fM_{f1} - a_4c_2M_{f1}^2)|\vec{q}_f|^2 \right. \\
& + (M_{f1} - a_4c_3M_{f1})\vec{q}_f \cdot \vec{P}_{f1} - a_4c_2|\vec{q}_f \cdot \vec{P}_{f1}|^2 + c_4(E_{f1}M_f - M_{f1}^2 + a_3M_f\vec{q}_f \cdot \vec{P}_{f1}) \\
& + |\vec{P}_{f1}|^2M_{f1}\alpha_2'' + (a_4c_2E_{f1} + M_{f1}a_3)(M_f - E_{f1})\vec{q}_f \cdot \vec{P}_{f1}\alpha_2'' + a_2(c_3M_{f1}(E_{f1} - M_f) \\
& \left. + c_2E_{f1}(\vec{q}_f \cdot \vec{P}_{f1} + |\vec{P}_{f1}|^2)\alpha_2'') \right\} \quad (B11)
\end{aligned}$$

- 
- [1] B. Aubert, *et al*, BABAR Collaboration, Phys. Rev. Lett 90 (2003) 242001.
  - [2] B. Aubert, *et al*, BABAR Collaboration, Phys. Rev. Lett 97 (2006) 222001.
  - [3] S. K. Choi, *et al*, Belle Collaboration, Phys. Rev. Lett 89 (2002) 102001.
  - [4] S. K. Choi, *et al*, Belle Collaboration, Phys. Rev. Lett 91 (2003) 262001.
  - [5] K. Abe, *et al*, Belle Collaboration, Phys. Rev. Lett 98 (2007) 082001.
  - [6] S. K. Choi, *et al*, Belle Collaboration, Phys. Rev. Lett 94 (2005) 182002.
  - [7] S. Uehara, *et al*, Belle Collaboration, Phys. Rev. Lett 96 (2006) 082003.
  - [8] B. Aubert, *et al*, BABAR Collaboration, Phys. Rev. Lett 95 (2005) 142001.
  - [9] P. del Amo Sanchez, *et al*, BABAR Collaboration, Phys. Rev. D 82 (2010) 111101.
  - [10] D. Ebert, R. N. Faustov, V. O. Galkin, Phys. Rev. D 82 (2010) 034019.
  - [11] Y.-M. Wang and C.-D. Lu, Phys. Rev. D 77 (2008) 054003.
  - [12] P. Colangelo, F. De Fazio and W. Wang, arXiv: 1009.4612 [hep-ph].
  - [13] I. Bediaga and J. H. Muñoz, arXiv: 1102.2190 [hep-ph].
  - [14] N. Isgur, D. Scora, B. Grinstein, M. B. Wise, Phys. Rev. D 39 (1989) 799.
  - [15] D. Scora, N. Isgur, Phys. Rev. D 52 (1995) 2783.
  - [16] D. Ebert, R. N. Faustov, V. O. Galkin, Phys. Rev. D 62 (2000) 014032.
  - [17] M. D. Pierro, A. K. Leibovich, e-Print: hep-ph/0207134.
  - [18] T. Nguyen, N. A. Souchlas, P. C. Tandy, AIP. Conf. Proc 1361 (2011) 142.
  - [19] A. Krassnigg, Phys. Rev. D 80 (2009) 114010.
  - [20] N. A. Souchlas, Phys. Rev. D 81 (2010) 114019.
  - [21] C.-H. Chang and G.-L. Wang, Science in China Series G 53 (2010) 2005.
  - [22] C.-H. Chang, J.-K. Chen and G.-L. Wang, Commun. Theor. Phys 46 (2006) 467.
  - [23] J.-M. Zhang, G.-L. Wang, Phys. Lett. B 684 (2010) 221.
  - [24] Z.-F. Sun, J.-S. Yu, X. Liu, T. Matsuki, Phys. Rev. D 82 (2010) 111501.
  - [25] X.-H. Zhong, Phys. Rev. D 82 (2010) 114014.
  - [26] B. Chen, L. Yuan, A. Zhang, Phys. Rev. D 83 (2011) 114025.
  - [27] D.-M. Li, P.-F. Ji, B. Ma, Eur. Phys. J. C 71 (2011) 1582.
  - [28] Z.-G. Wang, Phys. Rev. D 83 (2011) 014009.

- [29] C. S. Kim, G.-L. Wang, Phys. Lett. B 584 (2004) 285.
- [30] X.-J. Chen, H.-F. Fu, C. S. Kim, G.-L. Wang, Journal of physics G 39 (2012) 045002.
- [31] C. Long and D. Robson, Phys. Rev. D 27 644 (1983).
- [32] C.-H. Chang, C. S. Kim, G.-L. Wang, Phys. Lett. B 623 (2005) 218.
- [33] B. El-Bennich, M. A. Ivanov and C. D. Roberts, Phys. Rev. C 83 (2011) 025205.
- [34] A. Bender, C. D. Roberts and L. Von Smekal, Phys. Lett. B 380 (1996) 7, C. D. Roberts, Nucl. Phys. A 605 (1996) 475, D. Jarecke, P. Maris and P. C. Tandy, Phys. Rev. C 67 (2003) 035202, A. Höll, A. Krassnigg, P. Maris, C. D. Roberts and S. V. Wright, Phys. Rev. C 71 (2005) 065204, M. A. Ivanov, Yu. L. Kalinovsky and C. D. Roberts, Phys. Rev. D 60 (1999) 034018, M. A. Ivanov, J. G. Körner, S. G. Kovalenko and C. D. Roberts, Phys. Rev. D 76 (2007) 034018, M. A. Ivanov, Yu. L. Kalinovsky, P. Maris and C. D. Roberts, Phys. Rev. C 57 (1998) 1991, M. A. Ivanov, Yu. L. Kalinovsky, P. Maris and C. D. Roberts, Phys. Lett. B 416 (1998) 29.
- [35] P. Maris, C. D. Roberts and P. C. Tandy, Phys. Lett. B 420 (1998) 267, P. Maris and C. D. Roberts, Phys. Rev. C 56 (1997) 3369, C. J. Burden, C. D. Roberts and M. J. Thomson, Phys. Lett. B 371 (1996) 163.
- [36] S. Mandelstam, Proc. R. Soc. London 233 (1955). 248.
- [37] K. Nakamura *et al*, (Particle Data Group), Journal of physics G 37 (2010) 075021.
- [38] H.-F. Fu, G.-L. Wang, Z.-H. Wang, X.-J. Chen, Chin. Phys. Lett 28(12) (2011) 121301.
- [39] S. Ahmed, et al, Phys. Rev. Lett. 87 (2001) 251801; A. Anastassov, et al, Phys. Rev. D 65 (2002) 032003.
- [40] A. Abada, D. Becirevic, P. Boucaud, G. Herdoiza, J. P. Leroy, A. Leyaouanc, O. Pene, J. Rodriguez-Quintero, Phys. Rev. D 66 (2002) 074504.
- [41] D. Becirevic, B. Blossier, E. Chang and B. Haas, Phys. Lett. B 679 (2009) 231.
- [42] V. M. Belyaev, V. M. Braun, A. Khodjamirian and R. Rückl, Phys. Rev. D 51 (1995) 6177.
- [43] E.E. Salpeter and H.A. Bethe, Phys. Rev 84 (1951) 1232.
- [44] E.E. Salpeter, Phys. Rev 87 (1952) 328.